14th International Conference on Structural Safety and Reliability - ICOSSAR'25
1-6 June, 2025 - Los Angeles California, USA
R. Ghanem, E. Johnson, S. Masri and A. Olivier (Eds)

VINE-COPULAS-BASED STRUCTURAL MULTI-HAZARD RELIABILITY ASSESSMENT UNDER POST-EARTHQUAKE FIRE

Chen Zefan[1] **and Feng Decheng**[2]

[1] School of Civil Engineering, Southeast University
Nanjing 211189, China
zf-chen@seu.edu.cn

[2] Key Laboratory of Concrete and Prestressed Concrete Structures of the Ministry of Education, Southeast University
Nanjing 211189, China
dcfeng@seu.edu.cn

Key words: Post-earthquake fire, Reliability, Probabilistic analysis, Vine copulas

Abstract. Structural damage under multi-hazard conditions is much greater than that of a single hazard, and it is therefore urgent for researchers to consider the cascading effects between different hazards in the structural safety assessment. In this paper, a structural multi-hazard reliability analysis framework is proposed based on the vine copulas model. The framework is able to fully consider the nonlinear correlation between different hazards. A two-parameter failure criterion is used to reflect the failure mode of the structure under the combined effect of multiple hazards. A reinforced concrete (RC) structure is used as an illustrative example to validate the feasibility of the proposed approach. The structural failure probability p_f and reliability index β of structures under post-earthquake fire (PEF) scenario is investigated. The outcomes indicate that p_f and β exhibit increasing and decreasing trend as the increasing of intensities of earthquake and fire events. The developed framework can effectively characterizes nonlinear inter-dependencies among multi-hazard scenario, and provide a more accurate prediction of multi-hazard reliability of structures

1 INTRODUCTION

The concept of multi-hazard safety of structures has gained critical prominence in civil engineering research, driven by the cascading effects of multi-hazard scenarios that threaten critical infrastructure systems and socioeconomic stability. Historical cases demonstrate this complexity: Hanshin 1995 earthquake in Japen triggered widespread soil liquefaction, Wenchuan 2008 earthquake in China generated 257 landslide-dammed lakes and catastrophic debris flows, Tōhoku 2011 earthquake combined tsunamis with impact forces and fire propagation. More and more researchers recognize the compound impacts of sequential or interacting hazards as an existential threat to urbanized regions.

Traditional structural reliability analysis mostly focuses on single-hazard conditions [1, 2, 3]. Amirkardoust et al. [1] performed a seismic reliability analysis of RC structures using Monte Consideration sampling and nonlinear analysis with actual data from Tehran. Zhang et al. [2] proposed a reliability calculation framework based on Polynomial Chaos Expansion (PCE) to quantify the progressive collapse reliability index of RC structures under different failure column scenarios using

Pushdown analysis. The probability distribution of corrosion depth was derived via the corrosion test database by Stewart et al [3]. Based on this, the impact of corrosion spatio-temporal variability on the reliability of structures. Although existing literature have established some frameworks for reliability assessment of structures under different hazard conditions, the inter-hazard cascading failure mechanisms inherent to multi-hazard scenarios are neglected. The cumulative damage to the structure caused by the primary disaster weakens the load-bearing capacity of structures, and the further aggravation of the structural damage can lead to more serious consequences when the secondary disaster occurs. Therefore, it is necessary to propose a structural reliability analysis method that can take into account the correlation of disaster sequences. Moreover, the correlation of hazard intensities caused by multi-hazard sequences, as well as the complex nonlinearity and stochasticity between hazard intensities and structural damages also can not be overlooked. Traditional approach of structures subject to multiple disasters usually developed based on the linear assumption since the high computational complexity.

To address those issues, this study proposes a framework for calculating the multi-hazard reliability of structures. Vine-copulas model was adopted to consider the nonlinear correlation between the structural damage caused by primary and secondary disasters. The multi-hazed failure probability of structures was obtained by decomposition of the bi-variate conditional probability. A 4-story RC building with slabs exposed to PEF scenarios was investigated through the developed framework. Both failure probability and reliability index surfaces of the studied RC structure under PEF condition were derived.

2 MULTI-HAZARD RELIABILITY EVALUATION BASED ON VINE-COPULAS

2.1 Multi-hazard reliability definition

Structural reliability fundamentally refers to a structural capacity to maintain specified performance requirements throughout its service life under prescribed operating conditions. The reliability index R, geometrically quantified as the minimum distance from the origin to the limit state surface in standardized normal space, serves as a crucial metric in this assessment. The mathematical computation of structural reliability index typically involves direct integration of the joint probability density functions of random variables. However, two fundamental challenges emerge in practical engineering applications:

1. High dimensionality of required random variables complicates precise determination of comprehensive joint density functions.

2. Execution of multidimensional integration presents significant numerical challenges with substantial computational demands.

Consequently, the probabilistic relationships between reliability index and failure probabilities is employed to calculate the reliability index of structures in the engineering practice. This approach not only simplifies computational procedures but also maintains required accuracy thresholds for engineering applications. We assume the safety margin function of structures follows a normal distribution. Then, the structural reliability can be evaluated using:

$$\beta = \Phi^{-1}(1 - p_f) \tag{1}$$

where $\Phi^{-1}(\cdot)$ represents the standard normal distribution function, p_f is the probability of failure subject to multiple hazards.

For the multiple hazard issue, the cascading effects of sequential hazards necessitate explicit consideration of cumulative damage induced by the primary disaster. Hence, p_f becomes:

$$p_f = \Pr(\text{Collapse}|H_1 = h_1, H_2 = h_2) \tag{2}$$

where H_1 and H_2 are the primary and secondary disasters applied in structures, respectively, $\Pr(\cdot)$ stands for the bi-variate conditional probability given $H_1 = h_1$ and $H_2 = h_2$.

2.2 Multi-hazard failure probability calculation based on vine-copulas model

This section introduces the methodology for calculating the probability of failure under multiple disasters via vine-copulas model. The vine-copulas model was developed to create multivariate dependence structures using bi-variate copulas as foundational components. This model enables the recursive factorization of joint or conditional probability density functions (PDFs) for multivariate continuous distributions using bi-variate copula densities, marginal densities, and conditional distribution functions. Such process is called pair copula decomposition. It should be noted that this composition is not unique, however, all the possible composition construction have a conditional copula term, called pair copula.

The failure probability of structures subject to multiple hazards refers to the bi-variate conditional probability given primary and secondary disasters, which can be expressed as a three-dimensional copulas model, namely:

$$p_{3|12} = \frac{p_{23|1}(x_2, x_3|x_1)}{p_{2|1}(x_2|x_1)} \tag{3}$$

where $p_{23|1}(x_2, x_3|x_1)$ represents the conditional probability distribution function (PDF) of X_2 and X_3 given $X_1 = x_1$, $p_{2|1}(x_2|x_1)$ is the conditional PDF of X_2 given $X1 = x_1$.

The key step is how to obtain the $p_{23|1}(x_2, x_3|x_1)$ and $p_{2|1}(x_2|x_1)$ with consideration the nonlinear correlation between three required random variables X_1, X_2, and X_3. Sklaar proved the fundamental representation theorem, called ***Sklar's theorem***, say:

Let $\boldsymbol{X}= (X_1, \ldots, X_n)^T$ be a n-dimensional continuous random vector, assuming the corresponding joint probability distribution function is $F = (x_1, \ldots, x_n)$, and the marginal probability distribution functions for each dimension are $F_1(X_1), \ldots, F_n(x_n)$, then there be a unique function, $C(\cdot)$ satisfies:

$$F = (x_1, \ldots, x_n) = C(u_1, \ldots, u_n) \tag{4}$$

where

$$u_i = F_i(x_i), \text{ for } i = 1, \ldots, n. \tag{5}$$

where $C(\cdot)$ is copula function with copula density function $c(\cdot)$ as follows:

$$c(u_1, \ldots, u_n) = \frac{\partial C(u_1, \ldots, u_n)}{\partial u_1, \ldots, \partial u_n} \tag{6}$$

Based on Eq. (4), the joint probability density function of random vector $\boldsymbol{X}$ can be derived:

$$f(x_1, \ldots, x_n) = c(u_1, \ldots, u_n) \prod_{i=1}^{n} p_i(x_i), \text{ for } i = 1, \ldots, n. \tag{7}$$

where $p_i(x_i)$ represents the *i-th* dimensional marginal probability density function.

Hence, using Sklar's theorem, Eq. (3) becomes:

$$p_{3|12} = \frac{c_{23|1}(w_{2|1}, w_{3|1}) p_{2|1}(x_2|x_1) p_{3|1}(x_3|x_1)}{p_{2|1}(x_2, x_1)} = c_{23|1}(w_{2|1}, w_{3|1}) p_{3|1}(x_3|x_1) \tag{8}$$

where $c_{23|1}(w_{2|1}, w_{3|1})$ is the copula density function of conditional random parameters $X_2|X_1$ and $X_3|X_1$, $w_{s|r} = F_{r|s}(x_s, x_r)$, for $i = 1, 2, 3$, representing the conditional cumulative distribution function (CDF) of X_s given $X_r = x_r$. $p_{3|1}(x_3|x_1)$ denotes the conditional PDF of X_2 given $X_1 = x_1$, which can be written as:

$$p_{3|1}(x_3|x_1) = \frac{p_{13}(x_1, x_3)}{p_1(x_1)} = \frac{c_{13}(u_1, u_3) p_1(x_1) p_3(x_3)}{p_1(x_1)} = c_{13}(u_1, u_3) p_3(x_3) \tag{9}$$

where $c_{13}(u_1, u_3)$ is the copula density function of X_1 and X_2, and $u_q = F_q(x_q)$, for $q = 1, 2, 3$, is the uniform distribution on the interval $[0, 1]$.

Inserting Eq. (9) into Eq. (8), yielding:

$$p_{3|12}(x_3|x_1, x_2) = c_{23|1}(w_{2|1}, w_{3|1}) c_{13}(u_1, u_3) p_3(x_3) \tag{10}$$

2.3 Optimal selection of bi-variate copula functions

Copula functions are broadly classified into three principal families: elliptical, Archimedean, and Plackett. For this study, six bi-variate copula functions were selected to represent these categories: two elliptical copulas (Gaussian and Student's t-), three Archimedean copulas (Frank, Clayton, and Gumbel-Hougaard), and the Plackett copula. The corresponding copula density funcions are summarized in Table 1.

Table 1: Copula density functions

Copula	Copula density function
Gaussian[a]	$C_{2\|1}(v\|u) = \Phi\left(\frac{y-\lambda_{opt}x}{\sqrt{1-\lambda_{opt}^2}}\right)$
Student's t-[b]	$C_{2\|1}(v\|u) = T\left[(y-\lambda_{opt}x)\sqrt{\frac{v+1}{(v+x^2)\left(1-\lambda_{opt}^2\right)}}; \lambda_{dof}+1\right]$
Frank[c]	$C_{2\|1}(v\|u) = \frac{e^{-\lambda_{opt}u}\left(e^{-\lambda_{opt}v}-1\right)}{e^{-\lambda_{opt}}-1+\left(e^{-\lambda_{opt}v}-1\right)\left(e^{\lambda_{opt}u}-1\right)}$
Clayton[c]	$C_{2\|1}(v\|u) = u^{\lambda_{opt}}\left(u^{\lambda_{opt}-1}+v^{\lambda_{opt}-1}-1\right)^{1/\lambda_{opt}}$
Gumbel-Hougaard[d]	$C_{2\|1}(v\|u) = \frac{(-\ln u)^{\lambda_{opt}-1}}{v[g(u,v)]^{1-1/\lambda_{opt}}} e^{-[g(u,v)]^{1/\lambda_{opt}}}$
Plackett[c]	$C_{2\|1}(v\|u) = \frac{1}{2} - \frac{1+(\lambda_{opt}-1)(u+v)-2\lambda_{opt}v}{2\sqrt{[1+(\lambda_{opt}-1)(u+v)]^2-4\lambda_{opt}(\lambda_{opt}-1)uv}}$

[a] $x = \Phi^{-1}(u)$,$y = \Phi^{-1}(y)$, $0 \le \lambda_{opt} \le 1$, $\Phi(\cdot)$ is the Gaussian CDF.
[b] $x = T^{-1}(u; \lambda_{dof})$, $y = T^{-1}(v; \lambda_{dof})$, $0 \le \lambda_{opt} \le 1$, $\lambda_{dof} \ge 0$, $T(\cdot; \lambda_{dof})$ is the Student's t-CDF with the degree of freedom (DOFs) in λ_{dof}.
[c] $\lambda_{opt} > 0$
[d] $\lambda_{opt} \ge 1$, $g(u, v) = (-\ln u)^{\lambda_{opt}} + (-\ln v)^{\lambda_{opt}}$

Akaike proposed an approach to identify the optimal fitting copula function, which is called Akaike information criterion (AIC) [12]. The AIC formula is following:

$$\mathrm{AIC} = -2\sum_{j=1}^{N} \ln c_{r,s}\left(\tilde{u}_r^{(j)}, \tilde{u}_s^{(j)}; \lambda\right) + 2d_\lambda \tag{11}$$

where $c_{r,s}(\cdot)$ indicates an alternative copula density function of X_r and X_s, λ is the d_λ-dimensional optimal parameter vector of $c_{r,s}(\cdot)$ estimated by the maximum likelihood estimation (MLE) via observed samples, $\left(\tilde{u}_r^{(j)}, \tilde{u}_s^{(j)}\right)^T$ is the empirical probability distribution values of the *j-th* pair $\left(\tilde{x}_r^{(j)}, \tilde{x}_s^{(j)}\right)^T$ of observed samples of random vector $(X_r, X_s)^T$, namely:

$$\begin{aligned} \tilde{u}_r^{(j)} &= \frac{1}{N}\sum_{k=1}^{N} u\left(\tilde{x}_r^{(j)} - \tilde{x}_r^{(k)}\right) \\ \tilde{u}_s^{(j)} &= \frac{1}{N}\sum_{k=1}^{N} u\left(\tilde{x}_s^{(j)} - \tilde{x}_s^{(k)}\right) \end{aligned} \tag{12}$$

where $j = 1, \ldots, N$, $u(\cdot)$ represents the Heaviside's step function, N is the total number of pairs of observed samples of $(X_r, X_s)^T$.

The statistical goodness-of-fit for copula models is quantified through the magnitude of AIC values, where lower AIC values indicate stronger explanatory power in characterizing correlation between variables. Consequently, the copula density function achieving the minimal AIC value within the candidates is identified as the optimal one for the given dataset.

3 FRAMEWORK OF VINE-COPULAS BASED MULTI-HAZARD RELIABILITY

When structures are subjected to varying hazard scenarios, their performance characteristics diverge substantially due to distinct load-resisting mechanisms. This divergence becomes particularly pronounced for natural hazards inducing nonlinear quasi-static and dynamic responses, resulting in diverse damage measure selections. Hence, This section presents a systematic computational framework for assessing multi-hazard structural reliability through two damage criteria. Two distinct damage indices are integrated to address the structural performance degradation mechanisms considering the cascading effect of multiple disasters.

Step 1: Construction the sampled vector for primary and secondary hazards

Select the suitable responses parameters that describe the structural damage caused by primary and secondary disasters, which are denoted as RP_1 and RP_2, respectively. The corresponding hazard intensities are termed as $H_1 = h_1$ and $H_2 = h_2$, respectively. Construct the analyzed sampled vector of $(H_1, H_2, RP_1)^T$ and $(H_1, H_2, RP_2)^T$, both denoting as $\left(\tilde{x}_1^{(j)}, \tilde{x}_2^{(j)}, \tilde{x}_3^{(j)}\right)^T$, for $j = 1, \ldots, N$, where N is the sample size.

Step 2: Transformation empirical CDF

Assume random variables U_1, U_1, and U_3 follow a uniform distribution on the interval $[0, 1]$ and satisfy:

$$U_1 = F_{H_1}(X_1), U_2 = F_{H_2}(X_2), U_3 = F_{RP}(X_3) \tag{13}$$

Based on the sample vector , the mapped sample vectors $\left(\tilde{x}_1^{(j)}, \tilde{x}_2^{(j)}, \tilde{x}_3^{(j)}\right)^T$ and the empirical marginal CDFs of $(H_1, H_2, RP_m)^T$, for $m = 1, 2$, the mapped sample values $\left(\tilde{u}_1^{(j)}, \tilde{u}_2^{(j)}, \tilde{u}_3^{(j)}\right)^T$ of $(U_1, U_2, U_3)^T$ is obtained as:

$$\tilde{u}_s^{(j)} = \frac{1}{N} \sum_{k=1}^{N} u\left(\tilde{x}_s^{(j)} - \tilde{x}_s^{(k)}\right), \text{ for } s = 1, 2, 3, \text{ and } j = 1, \ldots, N. \tag{14}$$

Step 3: Determination the optimal copula functions for $C_{12}(\cdot)$ and $C_{13}(\cdot)$

The optimal copula parameters (λ_{opt}) of six copula function candidates can be derived based on the mapped sample values $(\tilde{u}_1^{(j)}, \tilde{u}_2^{(j)})^T$, for $j = 1, \ldots, N$ using MLE, that is the solution of d_λ-dimensional nonlinear equations system:

$$\frac{\partial}{\partial \lambda_{opt}} \sum_{j=1}^{N} \ln c_{12}\left(\tilde{u}_1^{(j)}, \tilde{u}_2^{(j)}; \lambda_{opt}\right) = 0 \tag{15}$$

Based on λ_{opt}, the optimal copula functions $c_{12}(u_1, u_2; \lambda_{opt})$ and $c_{13}(u_1, u_3; \lambda_{opt})$ can be determined by comparing the corresponding AIC values of the six copula function candidates.

Step 4: Determination the optimal copula function for $C_{23|1}(\cdot)$

Based on the sample values $\left(\tilde{u}_1^{(j)}, \tilde{u}_2^{(j)}, \tilde{u}_3^{(j)}\right)^T$ of $(U_1, U_2, U_3)^T$, for $j = 1, \ldots, N$, and the identified optimal copula functions $c_{12}(u_1, u_2)$ and $c_{13}(u_1, u_3)$, the sampled values corresponding to $W_{2|1} = F_{H_2|H_1}(H_2|H_1)$ and $W_{3|1} = F_{RP|H_1}(RP|H_1)$ can be obtained:

$$\begin{aligned} \tilde{w}_{2|1}^{(j)} &= C_{2|1}\left(\tilde{u}_2^{(j)} | \tilde{u}_1^{(j)}\right) \\ \tilde{w}_{3|1}^{(j)} &= C_{3|1}\left(\tilde{u}_3^{(j)} | \tilde{u}_1^{(j)}\right) \end{aligned} \tag{16}$$

where $j = 1, \ldots, N$. Then, the optimal copula function $c_{23|1}(w_{2|1}, w_{3|1})$ can be determined by repeating the same procedure of Step 3.

Step 5: Calculation of multi-hazard reliability index

By Step 1 to Step 4, marginal probability distribution of H_1, H_2, and RP_m, for $m = 1, 2$, can be derived by fitting the sample data vector $\left(\tilde{x}_1^{(j)}, \tilde{x}_2^{(j)}, \tilde{x}_3^{(j)}\right)^T$, for $j = 1, \ldots, N$. Then, the bi-variate conditional PDF $p_{RP_m|H_1,H_2}(rp_m|h_1, h_2)$, for $m = 1, 2$, can be obtained by inserting the previous obtained joint copulas into Eq. (10), i.e.,

$$\begin{aligned} p_{RP_m|H_1,H_2}(rp_m|h_1, h_2) = c_{23|1}\left\{C_{2|1}\left[F_{H_2}(h_2)|F_{H_1}(h_1)\right], C_{3|1}\left[F_{RP_m}(rp_m)|F_{H_1}(h_1)\right]\right\} \\ \cdot c_{13}\left[F_{H_1}(h_1), F_{RP_m}(rp_m)\right] \cdot p_{RP_m}(rp_m) \end{aligned} \tag{17}$$

As aforementioned, two different response parameters are employed to characterize the damage caused by primary and secondary hazards, leading to the multi-hazard failure probability consists of two failure probability calculated based on RP_1 and RP_2. Hence, the failure probability of structures exposed to multiple disasters under the given damage criteria reads:

$$p_f = \int_{DC_1||DC2}^{\infty} p_{RP_m|H_1,H_2}(rp_m|h_1, h_2) d(rp_m) \text{ for, } m = 1, 2. \tag{18}$$

where DC_1 and DC_2 represent the damage criteria based on RP_1 and RP_2, respectively.

Eq. (18) defines a compound failure criterion where structural collapse is triggered when either or both response parameters (RP_1 and RP_2) reach or exceed their considered thresholds. This inclusive logical condition (logical **OR** operation) ensures comprehensive coverage of all potential failure modes of multiple disasters. Following this failure criterion, the multi-hazard structural reliability can be evaluated by incorporating p_f into Eq. (1).

4 CASE STUDY: A RC BUILDING SUBJECT TO POST-EARTHQUAKE FIRE

4.1 Design of prototype structure

In this study, a 4-story RC structure designed following Chinese building codes [6, 7] was used to illustrate the proposed vine-copula-based multi-hazard reliability analysis methodology for the RC structures, as shown in Fig. 1. The structural performance under post-earthquake fire (PEF) was investigated. The span lengths of this RC structure are 6000 mm and 3000 mm. The height for the ground story is 4.5 m, whereas 3.5 m for the other. The dimensions of the beams and column are 500 $mm \times 250$ mm and 600 $mm \times 600$ mm, respectively. The slab thickness is 120 mm with two layers reinforcement rebar in x- and y- directions. The design dead load imposed on floor and roof are 5 kN/m^2 and 7 kN/m^2 respectively, the corresponding live loads both are 2 kN/m^2. The structure has a seismic design intensity of VII and a site class of II (the peak ground acceleration with a 10% probability of exceedance in 50 years is 0.10 g, where g≈9.8 m/s^2). The fire event was assumed to be occurred in only one compartment in the ground story, the columns, roof slab and beams were all exposed to fires, as shown in Fig. 1.

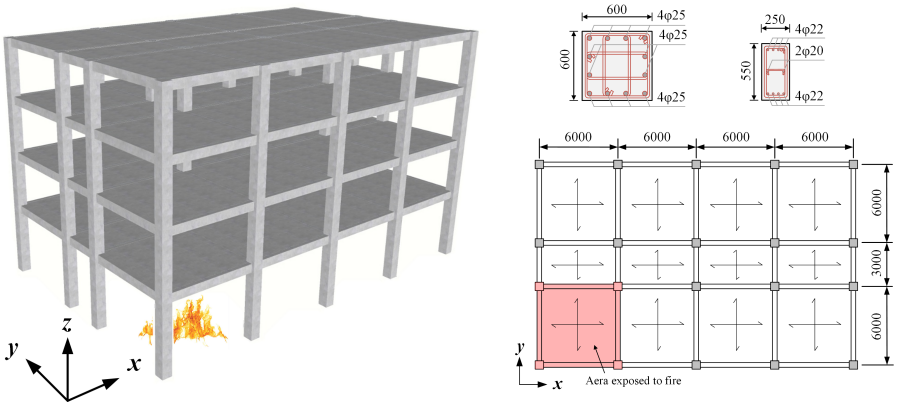

(a) Perspective view (b) Plan view

Figure 1: Design of 4-story RC structure (unit: mm)

4.2 Selection of ground motions and thermal loadings

To comprehensively account for hazard-induced uncertainties, a multi-hazard intensity measure (IM) matrix was established incorporating both seismic and thermal loading uncertainties. Seismic excitation inputs were derived from 160 horizontal ground motions curated from Baker's authoritative database [10], comprising 120 near-fault records and 40 near-fault pulse-type motions. All ground motion records were amplitude-scaled by 2.0 to ensure structural safety considerations under extreme events. For fire hazard, temperature (T) was adopted as the IM, with 320 distinct thermal exposure

scenarios generated through sampling of the ISO 834 standard time-temperature curve under uniform distribution. The integrated loading matrix combines 320 scaled ground motions with 320 T realizations.

4.3 Uncertainty consideration

Structural inherent uncertainties significantly influence the load-bearing capacity of structural systems. Hence, nineteen critical design parameters, including geometric dimensions and material properties, were selected to characterize these uncertainties, as shown in Table 2. The mean values of these variables were established as baseline Chinese design codes [6, 7], with corresponding coefficients of variation (COVs) and probability distributions rigorously defined by previous studies [11]. Latin hypercube sampling (LHS) was implemented to generate 320 sample points within $\pm$ 2 standard deviations of the mean values, thereby mitigating sampling bias. All variables were treated as mutually independent, with the sample size aligned to match the dimensionality of multi-hazard loading inputs.

Table 2: Random variables for the 4-story RC building

Random variable	Mean	Coefficient of variation	Distribution
Span length 1	6000 mm	0.3%	Normal
Span length 2	3000 mm	0.3%	Normal
Beam height	500 mm	1.0%	Normal
Beam width	250 mm	1.0%	Normal
Column width	600 mm	1.0%	Normal
Column length of ground story	4500 mm	0.3%	Normal
Column length of other stories	3500 mm	0.3%	Normal
Beam concrete cover thickness	30 mm	1.0%	Normal
Column concrete cover thickness	30 mm	1.0%	Normal
Slab concrete cover thickness	20 mm	1.0%	Normal
Slab thickness	120 mm	1.0%	Normal
Rebar diameter in beams	$22/20$ mm	4.0%	Normal
Rebar diameter in columns	25 mm	4.0%	Normal
Rebar diameter in slabs	10 mm	4.0%	Normal
Concrete compressive strength	26.0 MPa	18.0%	Lognormal
Concrete peak strain	0.002	15.0%	Lognormal
Concrete ultimate strain	0.02	52.0%	Lognormal
Yield strength of steel	400 MPa	7.4%	Lognormal
Elastic modulus of steel	200 GPa	3.3%	Lognormal
Rebar hardening ratio	0.02	20.0%	Lognormal

4.4 Optimal copula density function determination

The AIC values of six selected copulas functions for $(PGA, T, \theta_{max})^T$ and $(PGA, T, \xi_{max})^T$ were calculated and summarized in Tables 3 and 4, respectively. It is found that, for $(PGA, T, \theta_{max})^T$, the smallest AIC values for $C_{12}(\cdot)$, $C_{13}(\cdot)$, and $C_{23|1}(\cdot)$ were 0.46, -383.97, and -3.62, respectively,

resulting the best copulas function of Gumbel-Hougaard, Frank, and Gumbel-Hougaard, respectively. When it comes to $(PGA, T, \xi_{max})^T$, the Gumbel-Hougaard was adopted for both $C_{12}(\cdot)$ and $C_{13}(\cdot)$, Frank was identified for $C_{23|1}(\cdot)$, with corresponding AIC values of 0.46, 0.58, and -983.01, receptively.

Table 3: AIC values of $C_{12}(\cdot)$, $C_{13}(\cdot)$, and $C_{23|1}(\cdot)$ for $(PGA, T, \theta_{max})^T$

Copula	Gaussian	Student's t-	Frank	Clayton	Gumbel-Hougaard	Plackett
$C_{12}(\cdot)$	1.69	2.84	1.64	2.00	0.46	2.00
$C_{13}(\cdot)$	-317.73	-347.19	-383.97	-190.67	-354.78	-375.70
$C_{23\|1}(\cdot)$	-0.83	1.00	-2.28	-0.15	-3.62	2.84

Table 4: AIC values of $C_{12}(\cdot)$, $C_{13}(\cdot)$, and $C_{23|1}(\cdot)$ for $(PGA, T, \xi_{max})^T$

Copula	Gaussian	Student's t-	Frank	Clayton	Gumbel-Hougaard	Plackett
$C_{12}(\cdot)$	1.69	2.84	1.64	2.00	0.46	2.00
$C_{13}(\cdot)$	1.89	3.68	1.99	2.00	0.58	5.41
$C_{23\|1}(\cdot)$	-72.63	-939.76	-983.01	-549.64	-871.57	-884.98

4.5 Failure probability surfaces analysis

Cloud analysis methodology was employed to develop failure probability surfaces for the 4-story RC structure. The nonlinear time history analysis (NLTHA) and nonlinear static analysis (NLSA) were performed across 320 numerical models developed based on the generated dataset. Each of the 320 unique seismic-thermo loading scenarios was randomly assigned to 320 individual models via the Monte Carlo simulation principles. The maximum inter-stroy drift ratio (θ_{max}) and maximum vertical deflection ratio (ξ_{max}) were selected as the seismic- and fire-related response parameters, respectively. Four performance levels are used in this study according to FEMA 356 [4] and Chinese design codes [5], including normal operation (NO), immediate occupancy (IO), life safety (LS), and collapse prevention (CP). The corresponding thresholds for θ_{max} and ξ_{max} are provided in Table 5.

Table 5: Thresholds for θ_{max} and ξ_{max} under different limit sates

Limit state	NO	IO	LS	CP
θ_{max} (%)	0.18	0.50	1.50	4.00
ξ_{max} (%)	0.60	1.05	2.25	3.00

The multi-hazard failure probability surfaces of the 4-story RC building subject to PEF condition under different limit states are presented in Fig. 2. The results demonstrate that the failure probability

of the structure increases significantly with increasing PGA and T. Notably, the probability growth rates under seismic excitation exhibit descending magnitudes across the performance hierarchy: from NO through IO and LS to CP limit states. Thermal effects, however, exhibit comparatively stable probability increasing patterns. This thermal behavior stems from temperature-dependent material degradation mechanisms. Elevated temperatures induce rapid deterioration of material properties of concrete [8, 9], which directly compromises the load-resisting capacity of RC structures.

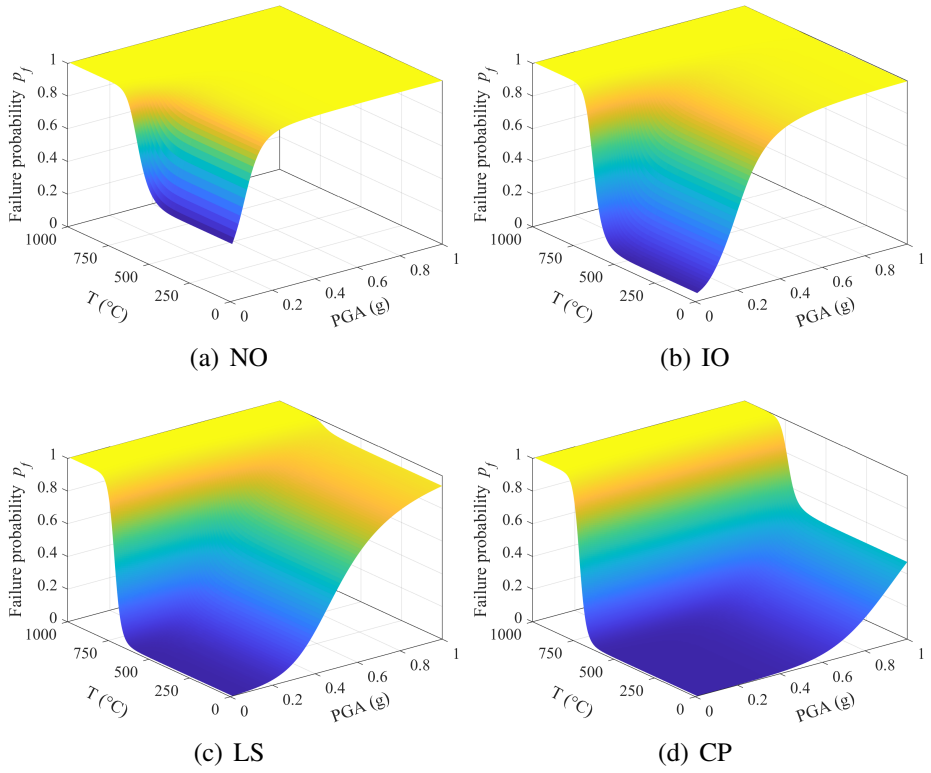

(a) NO (b) IO

(c) LS (d) CP

Figure 2: PEF failure probability surfaces under different limit states

4.6 Reliability index surfaces analysis

Based on the developed multi-hazard failure probability surfaces and Eq. (1), the reliability index surfaces of the 4-story RC building under under different limit states are derived, as plotted in Fig. 3. It is revealed that reliability index reductions across all four limit states as seismic and fire intensities increasing, an inverse relationship to the p_f trends presented in Fig. 2. Specifically, β of NO and IO demonstrate asymptotic stabilization under high-intensity seismic loading. Conversely, β of LS and CP maintain diminishing trends, albeit with attenuated reduction rates under the strong seismic hazard. Moreover, β relatively exhibits stable trend from T=0 °C to T≈500 °C, however, β undergoes accelerated deterioration when T approximately lager than 500 °C. For example, $\beta_{PGA=0.3g}$ for NO limit state when T=500 °C (end of the stable phase) and T=1000 °C (extreme thermal condition) are -2.25 and -6.32, respectively, with a reduction of 181%. The corresponding reductions in $\beta_{PGA=0.3g}$ values for IO, LS, and CP limit states are 634%, 467%, and 276%, respectively.

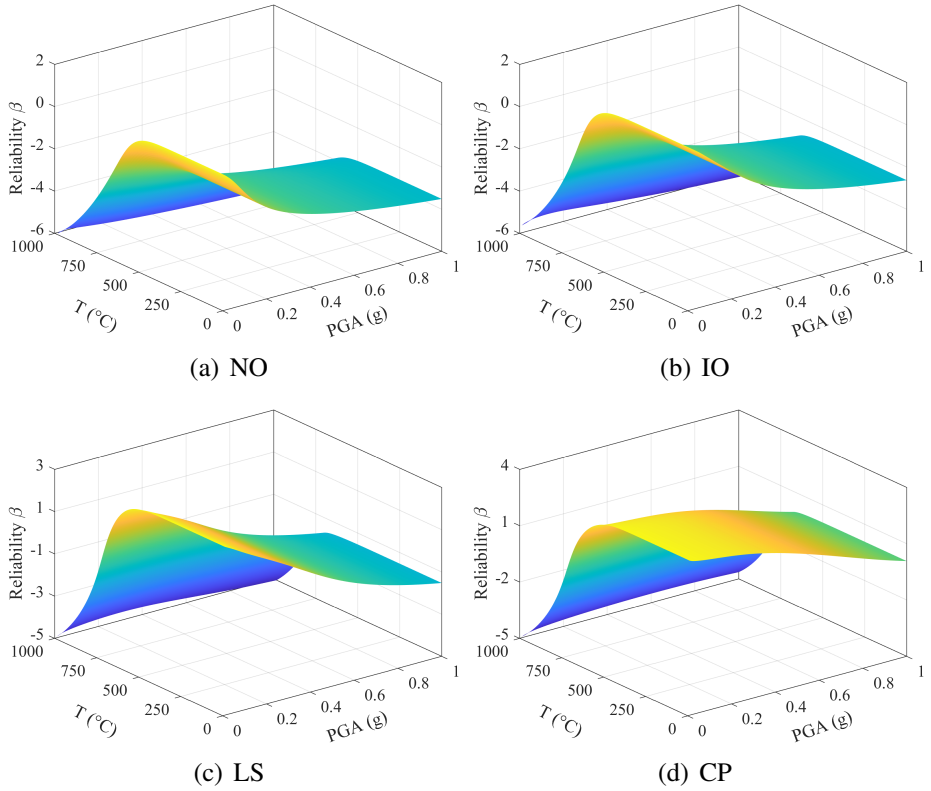

(a) NO (b) IO

(c) LS (d) CP

Figure 3: PEF reliability index surfaces under different limit states

5 CONCLUSIONS

This paper proposed a methodology to calculate the multi-hazard reliability of structures via vine-copulas model. The reliability of structures is calculated based on the multi-hazard failure probability under a normal distribution assumption. The vine-copulas model was adopted to fit the nonlinear relationship between the intensities of multiple disasters and responses parameter of structures. A 4-story RC building with slabs was investigated via the proposed approach. Both failure probability and reliability surfaces of the studied structure are derived. The general conclusion remarks drawn as follows:

- The paper provides a reliability assessment framework that effectively characterizes nonlinear inter-dependencies among multi-hazard scenarios, systematically considering the cascading effect of primary and secondary disasters. The developed framework can capture structural damage progression through dual-criteria response parameters, which reflects the combined failure mode induced by multiple hazard sequences.

- The multi-hazard failure probability (p_f) increases with the increasing magnitude of PGA and T. For all limit states, the growth velocities of p_F corresponding to increasing PGA and T are various. With the increasing of T, p_f show a a trend of stabilization followed by rapid increase under all limit states. However, the growth rates of p_F as the increasing PGA become smaller from NO to CP limit states.

- Multi-hazard reliability index of the studied RC structure decreases as seismic and fire intensities increasing. At low and medium temperatures, the change in reliability index of the studied RC structure is small, while at high temperatures, the sensitivity to temperature changes rises significantly. In contrast, seismic intensity has less impact on reliability index of the studied RC structure.

REFERENCES

[1] Amirkardoust, A., Hosseini, S.A., Seyedhosseini, S.M., Rabeifard, H., and Akbarpournickghalbrashti, A. Reliability assessment of reinforced concrete buildings using field data in Tehran. *J. Appl. Eng. Sci.* (2020) **10**:39–44.

[2] Zhang, Q., Zhao, Y.G., Kolozvari, K., and Xu, L. Reliability analysis of reinforced concrete structure against progressive collapse. *Reliab. Eng. Syst. Saf.* (2022) **228**:108831.

[3] Stewart, M.G., and Al-Harthy, A. Pitting corrosion and structural reliability of corroding RC structures: Experimental data and probabilistic analysis. *Reliab. Eng. Syst. Saf.* (2008) **93**:373–382.

[4] Federal Emergency Management Agency. (FEMA 356) *Prestandard and commentary for the seismic rehabilitation of buildings*. Council, Building Seismic Safety. (2000) Washington, DC.

[5] (CECS 392-2014), China Association for Engineering Construction Standardization. (CECS) *Code for anti-collapse design of building structures*. China Planing Press. (2014) Beijing, China. (in Chinese)

[6] (GB50010–2010), Ministry of Housing and Urban-Rural Development of the People's Republic of China. (MOHURD) *Code for design of concrete structures*. China Architecture and Building Press. (2010) Beijing, China. (in Chinese)

[7] (GB50011–2010), Ministry of Housing and Urban-Rural Development of the People's Republic of China. (MOHURD) *Code for seismic design of buildings*. China Architecture and Building Press. (2010) Beijing, China. (in Chinese)

[8] Chang, Y.F., Chen, Y.H., Sheu, M.S., and Yao, G.C. Residual stress–strain relationship for concrete after exposure to high temperatures. *Cem. Concr. Res.* (2006) **36**:1999–2005.

[9] Soc Concrete. *Assessment, design and repair of fire-damaged concrete structures*. The Concrete Society. (2008) London, Gamberley.

[10] Baker, J.W., Lin, T., Shahi, S.K., and Jayaram, N. *New ground motion selection procedures and selected motions for the PEER transportation research program*. PEER Report. University of California. (2011) Berkeley, CA.

[11] Celik, O.C., and Ellingwood, B.R. Seismic fragilities for non-ductile reinforced concrete frames—Role of aleatoric and epistemic uncertainties. *Struct. Saf.* (2010) **32**:1–12.

[12] Akaike, H.T. A new look at the statistical model identification. *IEEE Trans. Autom. Control* (1974) **19**:716–723.